UC Berkeley
UC Berkeley Previously Published Works

Title

Monoterpene 'thermometer' of tropical forest-atmosphere response to climate warming

Permalink

https://escholarship.org/uc/item/31g8t6qt

Journal

Plant Cell & Environment, 40(3)

ISSN

0140-7791

Authors

Jardine, Kolby J
Jardine, Angela B
Holm, Jennifer A
et al.

Publication Date

2017-03-01

DOI

10.1111/pce.12879

Peer reviewed

Original Article

Monoterpene '*thermometer*' of tropical forest-atmosphere response to climate warming

Kolby J. Jardine[1], Angela B. Jardine[2], Jennifer A. Holm[1], Danica L. Lombardozzi[3], Robinson I. Negron-Juarez[1], Scot T. Martin[4], Harry R. Beller[1,5], Bruno O. Gimenez[2], Niro Higuchi[2] & Jeffrey Q. Chambers[1,6]

[1]*Climate and Ecosystem Sciences Division, Lawrence Berkeley National Laboratory, 94720 Berkeley, CA, USA,* [2]*National Institute for Amazon Research (INPA), 69060-001 Manaus, Amazonas, Brazil,* [3]*Climate and Global Dynamics Laboratory, National Center for Atmospheric Research, 80307 Boulder, CO, USA,* [4]*Harvard University, School of Engineering and Applied Sciences, 02138 Cambridge, MA, USA,* [5]*Joint BioEnergy Institute, Lawrence Berkeley National Laboratory, 94068 Emeryville, CA, USA and* [6]*Department of Geography, University of California, 94720 Berkeley, CA, USA*

ABSTRACT

Tropical forests absorb large amounts of atmospheric CO_2 through photosynthesis but elevated temperatures suppress this absorption and promote monoterpene emissions. Using $^{13}CO_2$ labeling, here we show that monoterpene emissions from tropical leaves derive from recent photosynthesis and demonstrate distinct temperature optima for five groups (Groups 1–5), potentially corresponding to different enzymatic temperature-dependent reaction mechanisms within β-ocimene synthases. As diurnal and seasonal leaf temperatures increased during the Amazonian 2015 El Niño event, leaf and landscape monoterpene emissions showed strong linear enrichments of β-ocimenes ($+4.4\%\,°C^{-1}$) at the expense of other monoterpene isomers. The observed inverse temperature response of α-pinene ($-0.8\%\,°C^{-1}$), typically assumed to be the dominant monoterpene with moderate reactivity, was not accurately simulated by current global emission models. Given that β-ocimenes are highly reactive with respect to both atmospheric and biological oxidants, the results suggest that highly reactive β-ocimenes may play important roles in the thermotolerance of photosynthesis by functioning as effective antioxidants within plants and as efficient atmospheric precursors of secondary organic aerosols. Thus, monoterpene composition may represent a new sensitive 'thermometer' of leaf oxidative stress and atmospheric reactivity, and therefore a new tool in future studies of warming impacts on tropical biosphere-atmosphere carbon-cycle feedbacks.

Key-words: $^{13}CO_2$ labeling; drought; El Niño; heat; photosynthesis: carbon reactions; secondary organic aerosols; TPS synthase; volatile emissions.

INTRODUCTION

Tropical forests are estimated to be the largest global terrestrial carbon sink (Chambers *et al.* 2014), but are highly sensitive to climate change variables including warming and a reduction in precipitation. Regional-scale reductions in net primary

Correspondence: K. J. Jardine; e-mail: kjjardine@lbl.gov

productivity (NPP) and tree mortality associated with high temperature and drought are increasing in the tropics (Brienen *et al.* 2015; Laan-Luijkx *et al.* 2015; Lewis *et al.* 2011; Phillips *et al.* 2009; Zeng *et al.* 2008), with the physiological mechanisms through which tropical forests respond to climate warming under intense investigation. One of the earliest processes in plant response to abiotic stress is the rapid accumulation of reactive oxygen species (ROS) that initially function as warning signals that activate defense responses before triggering programmed cell death under excessive ROS accumulation (Mittler *et al.* 2011). Understanding how plants respond to oxidative stress is key to being able to predict (and perhaps mitigate) some of the resulting impacts on tropical forest biodiversity, structure and function as a globally important net carbon sink.

Recent literature suggests that isoprene and monoterpenes play roles in minimizing ROS accumulation through antioxidant mechanisms including physical membrane stabilization, the consumption of excess photosynthetic energy, direct antioxidant reactions and signaling properties of oxidation products (Jardine *et al.* 2016; Jardine *et al.* 2013; Karl *et al.* 2010; Loreto & Velikova, 2001; Morfopoulos *et al.* 2014; Schurgers *et al.* 2009; Singsaas *et al.* 1997; Vickers *et al.* 2009). Nevertheless, if stress is extended over a certain threshold, ROS production will overwhelm the scavenging action of the antioxidant system, resulting in membrane peroxidation and the reduction of ecosystem net primary productivity with a shift from terrestrial sinks to sources of atmospheric CO_2 (Brienen *et al.* 2015; Laan-Luijkx *et al.* 2015; Lewis *et al.* 2011; Phillips *et al.* 2009; Zeng *et al.* 2008). Such a shift in tropical forest carbon balance, as observed during the widespread 2005/10 droughts in the Amazon Basin (Feldpausch *et al.* 2016), eliminates a critical ecosystem service and accelerates global warming.

While the role of isoprene in thermotolerance of photosynthesis has been evaluated (Singsaas *et al.* 1997), little is known about the role of monoterpenes, despite several isomers possessing high reactivities with ROS (Jardine *et al.* 2015). Variations in monoterpene chemical structures strongly alter their biological activities and their chemical reactivities with ROS such as ozone (O_3) (Atkinson & Arey, 2003) and the

hydroxyl radical (OH·) (Arey *et al.* 1990). Whereas the reactivity of monoterpenes with ROS is poorly characterized in plants, their reactivity in the atmosphere affects air quality and climate through the formation/growth of secondary organic aerosols (Kavouras *et al.* 1999), which may act as effective cloud condensation nuclei (Pöschl *et al.* 2010). However, tropical leaf monoterpene emissions remain poorly studied, and global models assume tropical emissions are dominated by α-pinene (Guenther *et al.* 2012; Harley *et al.* 2014), which has moderate reactivity with ROS. Moreover, while emissions of monoterpenes are well known to increase with temperature, the composition is generally assumed constant. These assumptions are largely based on observations from temperate forests where monoterpene emissions typically derive from the evaporation from storage pools (Ghirardo *et al.* 2010), the extensive use of online methods unable to resolve monoterpene composition (Guenther *et al.* 2012; Harley *et al.* 2014), and the rarity of studies in the tropics, which are estimated by models to be the dominant global source of monoterpene emissions in the Earth system (Guenther *et al.* 1995). However, a single leaf study on the Mediterranean species *Quercus ilex* observed a temperature sensitivity of monoterpene emission composition. The highly reactive monoterpenes (E,Z)-β-ocimenes were hardly detected below 35 °C, but increased above this temperature at the expense of other isomers including (α,β)-pinene (Staudt & Bertin, 1998). To our knowledge, the temperature dependence of monoterpene emission composition has not been verified in other plants or studied in natural ecosystems.

Moreover, monoterpene emissions from broad leaf species are hypothesized to have similar environmental and physiological controls as isoprene (Jardine *et al.* 2015) including a strict dependence on light and the utilization of recent photosynthate as the principal carbon source (Karl *et al.* 2002). This was evaluated in a greenhouse study where *Q. ilex* leaves were fumigated with $^{13}CO_2$ and the ^{13}C-labeling of monoterpene emissions evaluated (Loreto *et al.* 1996). The authors reported ^{13}C-labeling patterns for the common monoterpene fragment detected at m/z 93 by gas chromatography–mass spectrometry (GC–MS). However, as this fragment contains only seven of the 10 total carbon atoms, a quantitative understanding of monoterpene carbon sources remains to be determined. Additionally, as has been well characterized for isoprene (Jardine *et al.* 2014; Jardine *et al.* 2016), the uncoupling of monoterpene emissions from net photosynthesis (Pn) at high leaf temperatures is anticipated as demonstrated by separate laboratory investigations of the Mediterranean species *Q. coccifera* (Staudt & Lhoutellier, 2011) and *Q. ilex* (Staudt & Bertin, 1998). In these studies, Pn had an optimum temperature significantly lower than that of monoterpene emissions. However, to-date this has not been demonstrated in tropical plants and field observations of this phenomenon are lacking.

In this study, as a part of the US Department of Energy (DOE) funded Next Generation Ecosystem Experiment (NGEE) Tropics project, we evaluated leaf monoterpene carbon sources and the temperature dependence of monoterpene emissions during record high leaf temperatures associated with a strong El Niño event during the 2015 dry season in central Amazonia. We first provide a quantitative

analysis of photosynthetic carbon sources for light-dependent monoterpene emissions from tropical leaves under a $^{13}CO_2$ atmosphere by determining the ^{13}C-labeling patterns of whole-monoterpene molecules containing all 10 carbon atoms. Secondly, we evaluate the role of controlled leaf temperature on individual monoterpene emissions from tropical leaves in relation to Pn in order evaluate how monoterpene emission rates and composition depend on leaf temperature. Next, we evaluate the role of naturally varying leaf temperature on monoterpene emission rates and composition at the leaf and landscape scales in a primary rain forest site in central Amazonia during diurnal and seasonal time scales as the forest transitioned between the wet and dry seasons during the strong 2015 El Niño event. Finally, we compare these observations with local and regional modeling estimates of the temperature dependence of monoterpene emission and composition from central Amazonia.

According to the established mechanism of monoterpene synthases (Chen *et al.* 2011; Degenhardt *et al.* 2009), multiple monoterpene products can be produced from a single enzyme *via* five distinct carbocation intermediates. Accordingly, we analysed temperature dependencies of monoterpene emission composition at the leaf and landscape scales throughout the 2015 El Niño in central Amazonia by placing monoterpenes into one of five groups corresponding to their individual carbocation precursor (Fig. 1). By calculating relative monoterpene emissions of each group, consistent temperature sensitivities emerged that were reproducible across large temporal (minutes to seasons) and spatial (leaves to landscape) scales.

MATERIALS AND METHODS

Monoterpene analysis by TD-GC–MC

Following air sample collection onto thermal desorption tubes, monoterpenes present in rain forest ambient air and leaf enclosure air samples were identified and quantified using thermal desorption gas chromatography mass spectrometry (TD-GC–MS) as previously described (Jardine *et al.* 2015) utilizing the dynamic solution injection method (Jardine *et al.* 2010) for regular calibrations with authentic liquid standards in methanol (Restek corp.). Monoterpenes in air samples at the leaf and landscape scales were collected in central Amazonia onto commercial thermal desorption tubes containing Quartz Wool, Tenax TA, and Carbograph 5TD adsorbents (QTC, Markes International) and analysed for 11 monoterpenes (Group 1: *E*-β-ocimene, *Z*-β-ocimene, β-myrcene; Group 2: α-pinene, β-pinene; Group 3: sabinene, β-thujene, γ-terpinene; Group 4: D-limonene and terpinolene; and Group 5: camphene) using a TD-GC–MS installed at the National Center for Amazon Research (INPA).

Carbon source analysis using $^{13}CO_2$

Whole molecule ^{13}C-labeling patterns of monoterpene emissions from banana leaves (*Musa* sp.) were studied as a function of photosynthetic active radiation (PAR, 0–2000 μmol m^{-2} s^{-1}) at a constant leaf temperature of 30 °C under a 500 mg g^{-1}
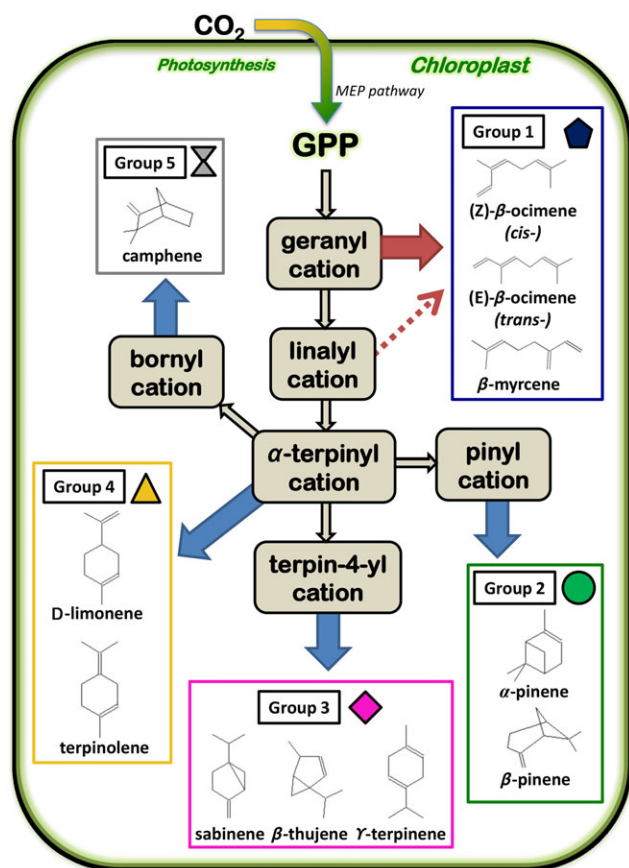
Figure 1. Schematic of temperature-dependent enzymatic mechanisms based on the AtTPS-Cin synthase of *Arabidopsis thaliana* (Chen *et al.* 2011; Degenhardt *et al.* 2009) showing the 11 monoterpenes observed in central Amazonia. Monoterpenes are grouped (Groups 1–5) according to their final carbocation intermediate. Grey boxes and arrows depict the enzymatic conversion of the photosynthetically derived substrate, geranyl pyrophosphate (GPP), to six carbocation intermediates. The solid blue arrows depict favoured lower leaf temperature mechanisms, while the solid and dotted red arrows represent favoured high leaf temperatures mechanisms. [Colour figure can be viewed at wileyonlinelibrary.com]

reference $^{13}CO_2$ atmosphere using the same experimental setup previously described for ^{13}C-isoprene labeling in *Manga indica* (Jardine *et al.* 2014). Once a new PAR intensity was reached, the LiCOR 6400 XT IRGAs were matched and a leaf was placed into the chamber. Gas-exchange measurements were recorded every 15 s for 10 min while leaf monoterpene emissions were collected on a single QTC tube at $100\,mL\,min^{-1}$ for 10 min. Analysis of QTC tube background samples collected without a leaf in the chamber at the beginning (PAR $0\,\mu mol\,m^{-2}\,s^{-1}$) and end (PAR, $2000\,\mu mol\,m^{-2}\,s^{-1}$) of the light curve showed negligible levels of monoterpenes. For each monoterpene at each level of PAR, relative emissions of monoterpene isotopologues (% total) were calculated by normalizing the peak area of a given monoterpene isotopologue by the total peak area. The following ions corresponding to monoterpene isotopologues with 0–10 ^{13}C-atoms were used for the analysis including m/z 136: $[^{12}C_{10}H_{16}]$, m/z 137: $[^{12}C_9^{13}C_1H_{16}]$, m/z 138: $[^{12}C_8^{13}C_2H_{16}]$, m/z 139:

$[^{12}C_7^{13}C_3H_{16}]$, m/z 140: $[^{12}C_6^{13}C_4H_{16}]$, m/z 141: $[^{12}C_5^{13}C_5H_{16}]$, m/z 142: $[^{12}C_4^{13}C_6H_{16}]$, m/z 143: $[^{12}C_3^{13}C_7H_{16}]$, m/z 144: $[^{12}C_2^{13}C_8H_{16}]$, m/z 145: $[^{12}C_1^{13}C_9H_{16}]$ and m/z 146: $[^{13}C_{10}H_{16}]$.

Leaf monoterpene temperature response

Coupled leaf monoterpene emissions and Pn responses for a leaf temperature range of 27.5 to 41.5 °C and constant PAR ($1000\,\mu mol\,m^{-2}\,s^{-1}$) were collected using a modified LiCOR 6400XT with a tee in the leaf chamber outflow to allow for the quantitative collection of monoterpenes on individual thermal desorption tubes (Jardine *et al.* 2015). Once a set point temperature was reached, the LiCOR 6400 XT IRGAs were matched and a leaf was placed into the chamber. Gas-exchange measurements were recorded every 15 s for 10 min while leaf monoterpene emissions were collected on a single QTC tube at $100\,mL\,min^{-1}$ for 10 min. Analysis of QTC tube background samples collected without a leaf in the chamber at the beginning (27.5 °C) and end (41.5 °C) of the temperature curve showed negligible levels of monoterpenes.

Diurnal gas-exchange in upper canopy leaves

Coupled photosynthesis-monoterpene emission measurements were performed on a *Pouteria anomala* individual growing near the K34 flux tower (60°12′33″W; 02°36′33″S) at the Reserva Biologica da Cuieiras (Jardine *et al.* 2015) in central Amazonia. Coupled leaf monoterpene emissions and Pn experiments were conducted on upper canopy *P. anomala* leaves accessible from the field site tower at a height of 25.5 m on 03, 12 and 29 September 2015 between 5:00–17:30 using the modified LiCOR 6400XT with a clear chamber top allowing natural variation in PAR levels during the sampling period. Prior to gas exchange measurements, a leaf temperature image of the *P. anomala* leaves to be studied was acquired at ~1 m distance using a NIST calibrated infrared camera (FLIR E5). The leaf temperature of the LiCOR 6400XT (empty enclosure) was set to match the observed leaf temperature. After the set point temperature was reached and the IRGAs matched, a background QTC thermal desorption tube air sample was collected at a constant flow rate of $155\,mL\,min^{-1}$ (ApexTM personal sampling pump, Casella) for 5 min. Following this, a leaf was placed inside the enclosure and gas exchange measurements were recorded every 15 s for 5 min. During this time, monoterpene emissions were quantitatively collected onto a QTC thermal desorption tube also with a flow of $155\,mL\,min^{-1}$. Following the 5-min sampling period, the leaf was removed from the chamber and the new leaf temperature set point was entered and the measurement cycle repeated. Throughout each of the three 12-h measurement periods, a total of 10–15 leaves were cycled through the modified LiCOR 6400XT system.

Diurnal ambient monoterpene concentrations

Natural 12-h patterns of ambient air monoterpene concentrations above the canopy were quantified for a primary rain forest at 27 m height on the K34 tower in central

Amazonia. In total, eight collections were made from 24 June–29 September 2015 using an automated volatile sampling system (Less-P, Signature Science). The Less-P autosampler was suspended directly underneath a platform on the K34 walkup tower to avoid exposure to direct sunlight and associated temperature anomalies from the tower. A 1.5 m length of 1/8 PFA Teflon tubing was attached to the Less-P inlet and mounted on a horizontal aluminium boom extending from the walkup tower. The Less-P was loaded with 27 QTC thermal desorption tubes and programmed to sequentially collect air samples at $100\,mL\,min^{-1}$ for 30 min on tube 2–26 starting at 5:00 and ending at 17:30 LT. Air samples were not collected on tube 1 and tube 27, which were used to demonstrate the lack of monoterpenes without air sample collection. Following the return to the laboratory, the 27 QTC tubes were removed from the Less-P and analysed for monoterpenes by TD-GC–MS. An example extracted ion chromatogram ($m/z = 93$) from the ambient air showing the presence of 11 different monoterpenes above the upper canopy (27 m) on the K34 tower is shown in Fig. S1. Half hour ambient air diurnal monoterpene concentrations above the canopy were compared with leaf surface temperature determined with an infrared radiometer (SI-111, 22° half angle field of view, Apogee Inst.) installed on the K34 tower and aimed at a group of branches at the top crown of the *P. anomala* tree (25.5 m height).

Volumetric water content

Two soil moisture profiles were installed in 1 m deep pits at 20 m to the northeast and 25 m to the south of the K34 tower. The soil moisture profiles were measured using soil water content reflectometer (CS655 12 cm, Campbell SCI) placed at 10, 20, 40, 60 and 100 cm deep. Measurements were collected every 30 min. The sensors measure the dielectric permittivity that is then converted to soil moisture (m^3/m^3) using the Topp equation (Topp *et al.* 1980).

Coupled MEGAN 2.1 – Community Land Model 4.5 models

We used the Model of Emissions of Gases and Aerosols from Nature (MEGAN 2.1) (Guenther *et al.* 2012) embedded in a biogeochemistry land surface model, the Community Land Model (CLM 4.5) (Oleson *et al.* 2010) to evaluate how a cutting edge Earth System Model predicts monoterpene emissions in central Amazonia at the landscape (single 1° × 1° grid cell) and regional (5° × 5°) scales. At the landscape scale, monoterpene emissions were simulated as hourly averages across a 24-h period for the month of September 2008 in relationship to leaf surface temperature and net primary production in a 1° × 1° grid cell centred at 60°0′0″W, 2°21′36″S and encompassing the K34 tower. The model was forced with site-specific meteorological data taken from the K34 field site flux tower for September 2008, with 2008 being the latest year of recorded, obtainable data. We previously demonstrated that

CLM 4.5 fails to capture the upper ~12 °C of leaf temperatures for central Amazonia. Therefore, a scenario that allowed for higher leaf temperatures (where 12 °C was added to all model forced leaf surface temperatures), was simulated for September 2008 in addition to the default MEGAN-CLM set-up to directly compare with this study's observations.

The 5° × 5° regional CLM 4.5 simulation encompassed the central Amazon Basin Northwest corner: 72°0′0″W, 5°5′60″S Southeast corner: 58°0′0″W, 13°54′0″S using the supported 5° × 5° Amazon grid that was released with the CLM4.5. The simulation was run using the Climate Research Unit (CRU)-National Centers for Environmental Prediction (NCEP) climate forcing data (downloaded from http://dods.ipsl.jussieu.fr/igcmg/IGCM/BC/OOL/OL/CRU-NCEP/). The CRU-NCEP climate forcing data combines the CRU time series 3.1 (TS3.1) 0.5° × 0.5° monthly climatology with the NCEP-National Center for Atmospheric Research (NCAR) reanalysis 2.5° × 2.5° 6-hourly climatology to generate a historical atmospheric dataset of observed precipitation, temperature, specific humidity, air pressure, surface wind speed and downward solar radiation. The regional simulation was run from 1950 to 2010 and generated monthly average values. Analysis focused on the year 2005, as this was a strong drought period in the Amazon Basin.

RESULTS

Leaf carbon source analysis under $^{13}CO_2$

Leaf monoterpene emissions from banana (*Musa* sp.) were investigated under a $500\,mg\,g^{-1}$ $^{13}CO_2$ atmosphere during controlled light curves for which photosynthetically active radiation (PAR) was varied between 0 and $2000\,\mu mol\,m^{-2}\,s^{-1}$ at a constant leaf temperature (30 °C). In the dark, completely ^{13}C-labeled monoterpene emissions $[^{13}C_{10}H_{16}]$ were not detected, but were observed at the lowest light intensity (PAR of $100\,\mu mol\,m^{-2}\,s^{-1}$). Absolute emissions of $[^{13}C_{10}H_{16}]$ increased without saturation for each of the 10 monoterpenes identified [β-thujene, α-pinene, camphene, sabinene, β-pinene, (E)-β-ocimene, D-limonene, (Z)-β-ocimene, γ-terpinene and terpinolene] up to the highest light intensity studied (Fig. 2a). While absolute $[^{13}C_{10}H_{16}]$ emissions of each individual monoterpene continued to increase with light intensity, relative emissions (% total monoterpene isotopologues) remained essentially constant at light intensities above $1000\,\mu mol\,m^{-2}\,s^{-1}$. When averaged for the eight highest emitted monoterpenes [α-pinene, camphene, sabinene, β-pinene, (E)-β-ocimene, D-limonene, (Z)-β-ocimene and terpinolene] at maximum light intensity (Fig. 2b), $64.0 \pm 5.6\%$ of monoterpene emissions were completely ^{13}C-labled $[^{13}C_{10}H_{16}]$ while $92.0 \pm 5.8\%$ of monoterpene emissions had between eight and 10 ^{13}C-atoms $([^{13}C_8^{12}C_2H_{16}] + [^{13}C_9^{12}C_1H_{16}] + [^{13}C_{10}H_{16}])$. Therefore, nearly all monoterpenes emitted from banana under a $500\,mg\,g^{-1}$ $^{13}CO_2$ atmosphere were ^{13}C-labeled, with the majority completely ^{13}C-labeled. These observations are consistent with the use of recently assimilated geranyl pyrophosphate
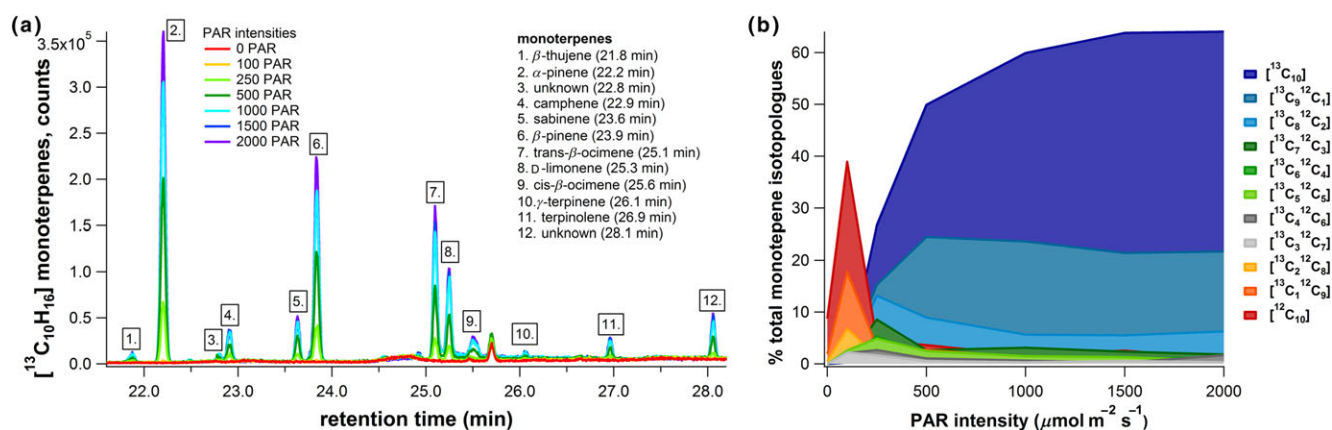
Figure 2. (a) Extracted ion (m/z = 146) chromatogram of leaf volatile emissions from *Musa* sp. as a function of PAR (0–2000 $\mu mol\,m^{-2}\,s^{-1}$) under a 500 mg g^{-1} reference $^{13}CO_2$ atmosphere showing whole molecule ^{13}C-labeling of 12 individual monoterpenes ($^{13}C_{10}H_{16}$). (b) Relative abundance of ^{13}C-monoterpene isotopologue emissions (% total) as a function of PAR emitted from *Musa* sp. are shown for the eight dominant monoterpenes (α-pinene, camphene, sabinene, β-pinene, (E)-β-ocimene, D-limonene, (Z)-β-ocimene and terpinolene). [Colour figure can be viewed at wileyonlinelibrary.com]

(GPP), as the common substrate used by monoterpene synthases (Fig. 1).

Controlled temperature monoterpene emissions

Controlled leaf temperature experiments on banana leaves under constant light intensity (PAR of $1000\,\mu mol\,m^{-2}\,s^{-1}$) showed individual monoterpene emissions with distinct temperature optima (Fig. 3a). For example camphene emissions peaked at 37 °C, (α,β)-pinene peaked at 40 °C and (E,Z)-β-ocimene emissions continued to increase up to the maximum temperature (42 °C). Individual monoterpene emissions within each of the five groups were highly correlated and when normalized by the total emissions, followed distinct positive or negative temperature responses patterns (Fig. 3b). For example, while total monoterpene emissions increased with leaf temperature ($1.5\,nmol\,m^{-2}\,s^{-1}\,°C^{-1}$), Group 1 relative

emissions (% total) showed a positive temperature sensitivity ($+1.1\%\,°C^{-1}$) while Group 2 ($-1.0\%\,°C^{-1}$) and Group 4 ($-0.1\%\,°C^{-1}$) showed negative temperature sensitivities. Groups 3 and 5 had low emission rates (<2.7%), and showed negligible temperature sensitivities (Fig. 3c). Resulting slopes and linear R^2 coefficients of determination for all temperature sensitivity analyses can be found in Table 1.

Additionally, an uncoupling of total monoterpene emissions from net photosynthesis (Pn) occurred. While Pn reached a maximum of $21\,\mu mol\,m^{-2}\,s^{-1}$ at 32.5 °C and declined at higher temperatures, total monoterpene emissions continued to increase with temperature, reaching a maximum of $21\,nmol\,m^{-2}\,s^{-1}$ at 40 °C and slightly declining at 42 °C (Fig. 3b). Thus, a strong linear temperature sensitivity of monoterpene emission composition was observed from banana leaves with (α,β)-pinene (Group 2), the assumed dominant monoterpene in tropical ecosystems, showing a negative
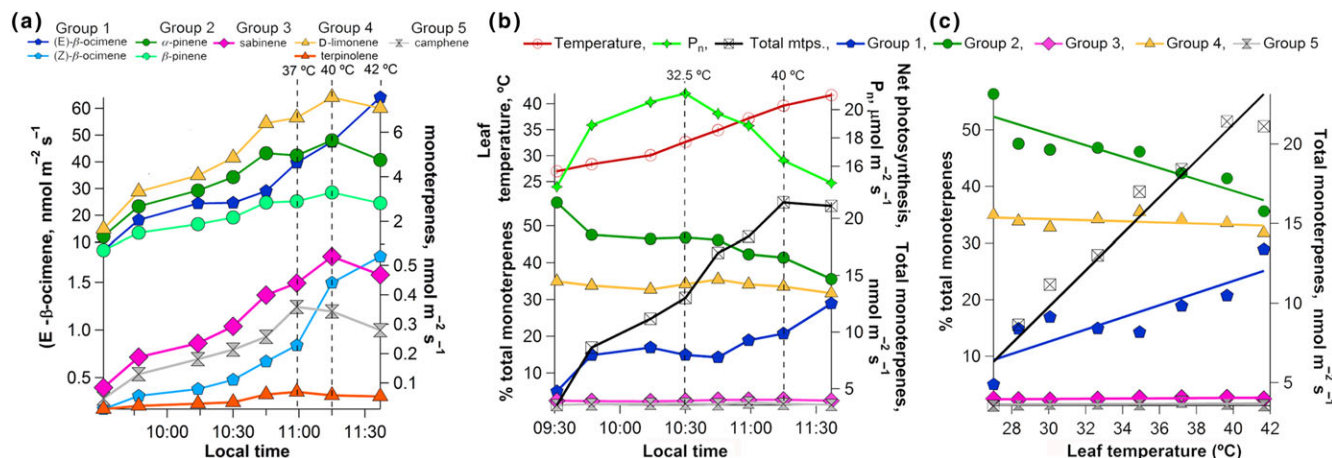

Figure 3. (a) Absolute leaf monoterpene emissions during a leaf temperature curve under constant light intensity (PAR of $1000\,\mu mol\,m^{-2}\,s^{-1}$) from an intact *Musa* sp. leaf. (b) Leaf temperature, net photosynthesis (Pn) response, total monoterpene emissions and Groups 1–5 monoterpene composition (% total) during a leaf temperature curve. (c) Groups 1–5 monoterpene composition as a function of leaf temperature. See Table 1 for slopes and linear R^2 coefficients of determination. Dashed vertical lines indicate leaf temperature optima of individual monoterpene emissions. [Colour figure can be viewed at wileyonlinelibrary.com]

Table 1. Temperature sensitivities (% total°C^{-1}) for Groups 1–5 monoterpene emissions together with respective coefficients of determination from linear regression analyses (R^2, shown in parentheses) for observations at the leaf and landscape scales and model results at the landscape and regional scales. Note the inability of the model to capture the positive temperature sensitivity of Group 1 monoterpenes and the negative sensitivity of Group 2–4 monoterpenes.

Figure	Experiment	Group 1	Group 2	Group 3	Group 4	Group 5
3c	Leaf (*Musaceae* sp.)	+1.1 (0.2)	−1.0 (0.8)	0.0 (0.4)	−0.1 (0.2)	0.0 (0.1)
S2b	Leaf (*P. anomala*, 5:00–17:30) 12 Sept. 2015	+4.4 (0.4)	−0.1 (0.0)	−3.5 (0.4)	−0.5 (0.0)	−0.2 (0.0)
S2d	Landscape (5:00–17:30) 12 Sept. 2015	+1.5 (0.6)	−0.3 (0.1)	+0.1 (0.1)	−1.3 (0.5)	+0.0 (0.0)
5b	Landscape, (11:00–11:30) 24 June to 29 Sept. 2015	+4.4 (0.8)	−0.8 (0.2)	−0.9 (0.2)	−2.9 (0.6)	+0.1 (0.9)
6b	Modeled landscape, Sept. 2008	−0.2 (0.8)	+0.4 (0.8)	+0.1 (0.8)	−0.2 (0.8)	0.0 (0.8)
6d	Modeled region, Year 2005	−0.1 (0.8)	+0.2 (0.8)	0.0 (0.8)	−0.1 (0.8)	0.0 (0.8)

sensitivity and the highly reactive monoterpenes (*E,Z*)-*β*-ocimene (Group 1) showing a positive sensitivity.

Diurnal leaf and landscape monoterpene emissions during the 2015 El Niño

The 2015 dry season in central Amazonia was associated with a strong El Niño event marked by anomalously warm leaf surface temperatures. At the landscape scale (1° × 1°), satellite observations from the Atmospheric Infrared Sounder (AIRS) revealed September 2015 was the warmest monthly averaged

surface air temperature over the past 13 years (Fig. 4a). Daytime air temperatures in September were nearly 1.0 °C warmer than any month in 2005 or 2010, the two most recent Amazon drought years (Lewis *et al.* 2011; Marengo *et al.* 2011). At the field site, maximum daytime leaf surface temperatures of upper canopy leaves increased throughout the dry season from a maximum of 30–35 °C during the early dry season (June–July 2015) to 40–42 °C by the late dry season (September 2015) (Fig. 4b). Strong diurnal leaf temperature increases on 29 September 2015 were verified using a thermal imaging camera, which observed maximum leaf temperatures in the upper canopy up to 44.5 °C by 14:00 (Fig. 4c). The
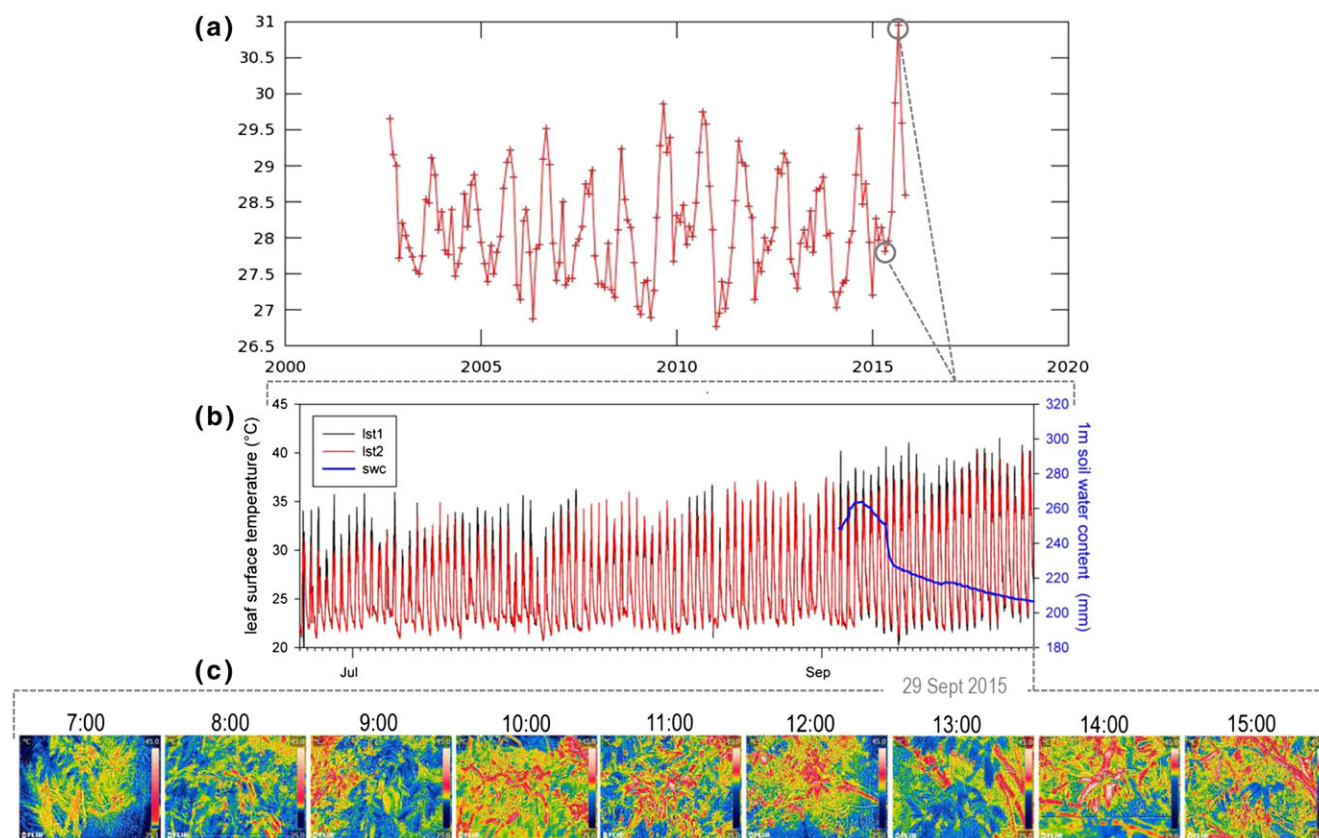

Figure 4. (a) Landscape scale monthly averaged air surface temperatures (°C) for the field site for the period September 2002–November 2015; AIRS AIRX3STM v 006. (b) Observations at the field site tower during the study period 24 June 2015–29 September 2015 for leaf surface temperatures at 24 m (lst1) and 22 m (lst2) and 1 m integrated soil water content (swc, mm) for the month of September 2015. (c) Diurnal lst images of *P. anomala* branches at 25.5 m on 29 September 2015. [Colour figure can be viewed at wileyonlinelibrary.com]

historically high air and leaf temperatures during September were associated with a lack of significant precipitation after September 3. Consequently, soil water content integrated across the first 1 m at the field site decreased by 22% during September (Fig. 4b).

A representative diurnal pattern of leaf trace gas exchange from *P. anomala* is shown for September 12 (Fig. S2a). In the early morning, net photosynthesis (Pn) rates and total monoterpene emissions increased together with leaf temperature. Pn reached a maximum of 12.1 μmol m^{-2} s^{-1} at 09:30 LT (34.3 °C), whereas total monoterpenes continued to increase with leaf temperature reaching a maximum of 1.5 nmol m^{-2} s^{-1} at 39.6 °C by 10:30. Thus, an uncoupling of total monoterpene emissions and Pn was observed at high temperatures; this phenomenon was also observed on September 3 and 29. During the first 2 h on September 12, when total emissions were low and leaf temperatures climbed steadily to 29.9 °C by 08:00, monoterpene emissions were dominated by Group 3, which represented up to 70% of total emissions. However, by 08:30 leaf temperatures reached 32.8 °C and Group 3 monoterpenes declined to 2% of total emissions while Group 1 monoterpenes increased to 97% of total emissions (Fig. S2a). For the rest of the day, Group 1 monoterpenes composed 95 ± 4% of total monoterpene emissions, whereas Group 3 composed only 4 ± 3%. However, when leaf temperatures decreased at the end of the afternoon, total monoterpene emissions strongly declined and Group 3 relative emissions showed a slight recovery (1 to 4%) with a corresponding decrease in Group 1 relative emissions. A similar relationship between Group 3-dominated monoterpene emissions at lower temperatures and Group 1 dominated emissions at higher temperatures was also observed for *P. anomala* leaves on 03 and 29 September 2015. When all 3 days of data were pooled in September, total leaf monoterpene emissions increased linearly with leaf temperature (0.1 nmol m^{-2} s^{-1} °C^{-1}) while monoterpene composition changed linearly. Relative emissions of Group 1 monoterpenes increased at +4.4% °C^{-1} while Group 3, Group 4 and Group 5 declined at −3.6, −0.5 and −0.2% °C^{-1}, respectively (Fig. S2b).

Further, we sampled ambient air above the main canopy between 5:00 and 17:30 on eight separate days from 25 June–29 September 2015 (Fig. S2c for 12 September 2015). On 12 September 2015, total ambient monoterpene concentrations increased throughout the morning with leaf temperature, reaching a maximum of 3.0 ppb at 10:00 and remaining variable but elevated throughout the afternoon. During this period, the relative composition of Group 1 monoterpenes steadily increased from 11% at 05:00 to a maximum of 42% at 13:00 when leaf temperature also reached a maximum of 35 °C. As temperatures increased, Groups 2 and 4 generally decreased in relative abundance whereas and Groups 3 and 5 remained low and variable. Ambient concentrations of Group 5 monoterpenes could be detected but remained low throughout the day (<2.7%). When regressed against leaf surface temperature, total ambient monoterpene concentrations showed positive linear correlations (+0.1 ppb °C^{-1}, Fig. S2d). As observed at the leaf level, landscape scale monoterpene composition changed

linearly as a function of leaf temperature. Group 1 ambient monoterpenes showed a positive temperature sensitivity (+1.5% °C^{-1}), while Groups 2 and 4 had negative sensitivities (−0.3 and −1.3% °C^{-1}, respectively). Group 3 showed a slight positive temperature sensitivity (+0.1% °C^{-1}) while Group 5 showed no sensitivity to temperature.

At the leaf and landscape scales during September 2015, Group 1 monoterpenes composed the majority of midday leaf emissions and ambient concentrations and showed a positive increase in relative abundance with temperature while Group 2 and 4 monoterpenes showed negative temperature sensitivities at both scales. However, the ambient air showed higher relative abundances of Group 2 and 4 monoterpenes compared with leaf emissions. Group 3 monoterpenes remained below 7% of the ambient air monoterpene composition, but made up to 64% of the monoterpene composition in leaf emissions at low temperatures. Thus, the emissions from *P. anomala* leaves cannot solely explain the landscape scale ambient concentration observations, which are impacted by a large footprint. Nonetheless, the results suggest that all monoterpene emitting trees contributing to the ambient air within the tower footprint show a positive temperature sensitivity of Group 1 monoterpene emissions and a corresponding negative temperature sensitivity for Groups 2–4 (with small to negligible emission of Group 5 monoterpenes).

Seasonality of monoterpene composition

Mid-day ambient monoterpene concentrations and composition above the primary rain forest canopy were analysed across the early to late dry season in 2015 in central Amazonia (Fig. 5). The time period 11:00–11:30 was chosen as early afternoon periods often showed considerable cloud cover, particularly in the early dry season. Half hour averaged leaf temperatures (Fig. 5a) increased from 27.3 °C on 25 June 2015 to 35.5 °C on 29 September 2015. Likewise, total monoterpene ambient concentrations doubled from 1.5 ppb on 25 June 2015 to 3.0 ppb on 29 September 2015. Group 1 contributions to the total ambient monoterpene concentrations above the canopy increased from a minor component of the total (12.7%) during the early dry season on 25 June 2015, to the dominant monoterpene group (48.2%) during the late dry season on 29 September 2015. The dominance of Group 1 monoterpenes in the ambient air above the canopy occurred throughout the month of September (Fig. 5a) coinciding with the highest remotely sensed air temperature estimates recorded over the 13-year AIRS time series (Fig. 4a). Similar to leaf level emissions (Fig. 3c and S1b), the relative composition of Group 1 monoterpenes at the landscape level showed a strong positive linear sensitivity to temperature (+4.4% °C^{-1}), which was balanced by negative temperature sensitivities of Group 2–4 monoterpenes (Fig. 5b). Group 5 monoterpenes showed a small to negligible temperature sensitivity (+0.1 % °C^{-1}).

MEGAN 2.1 – Community Land Model 4.5 models

MEGAN 2.1-CLM 4.5 monoterpene emissions for central Amazonia were simulated as hourly averages at the landscape
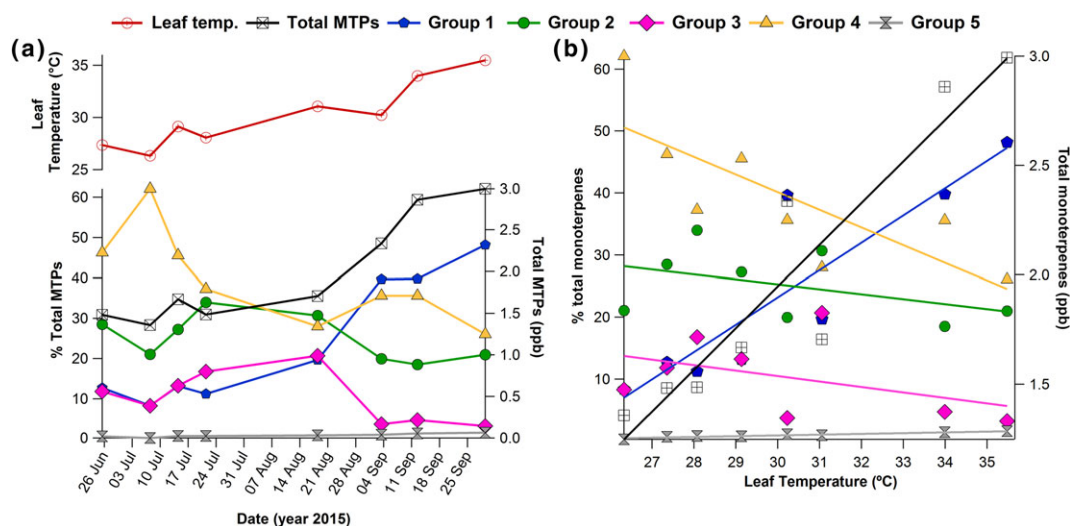
Figure 5. Seasonal patterns of landscape monoterpene emission composition in central Amazonia across the wet-dry season transition (25 June–29 September 2015). (a) Seasonal variation in mid-day [11:00–11:30 (LT)] leaf temperature together with total monoterpene (MTPs) ambient concentrations and composition (Groups 1–5, % total) above the main canopy (27.0 m) (b) Total mid-day monoterpene ambient concentrations and composition plotted as a function of leaf temperature. See Table 1 for slopes and linear R^2 coefficients of determination. [Colour figure can be viewed at wileyonlinelibrary.com]

scale overlapping with the field site tower, and as monthly averages at the regional scale (see map in Fig. S3). Diurnal simulations at the landscape scale (Fig. 6a) and annual simulations at the regional scale (Fig. 6c) showed a tight coupling between leaf temperature and total monoterpene emissions, which reached maximum values in the early afternoon and the late dry season in September–October, respectively. Like the central Amazonia field observations at the leaf and landscape scales, modeled total monoterpene emissions at both scales increased linearly with leaf temperature (Fig. 6b,d). Unlike the observational field data, modeled monoterpene emission composition was insensitive to large diurnal and seasonal temperature variations. As summarized in Table 1, the model was unable to predict the strong positive temperature sensitivity of Group 1 monoterpenes and the corresponding negative temperature sensitivity of Groups 2–4. Thus, the model predicted a constant dominance of Group 2 monoterpenes ($61 \pm 1\%$), whereas actual field observations showed Group 2 monoterpenes declined in relative abundance to 21% during September 2015. Likewise, the model predicted a small and constant contribution of Group 1 monoterpenes ($21 \pm 0.1\%$); while field observations revealed that they dominated emissions (48.2%) during September 2015. These results demonstrate the large overestimation of Group 2 monoterpenes at high temperatures by the model at diurnal to seasonal temporal scales and from landscape to regional spatial scales. However, as observed in the field data, the model captures the low relative emissions of Group 5 monoterpenes and its lack of temperature sensitivity.

DISCUSSION

Although evidence is lacking, tropical leaf monoterpene emissions are expected to have similar environmental and physiological controls as isoprene. This includes a strict dependence

on light and the utilization of recently assimilated carbon as the principal carbon source (Karl *et al.* 2002). Under a $^{13}CO_2$ atmosphere, Mediterranean *Q. ilex* leaves showed strong ^{13}C-labeling of the common C_7 monoterpene fragment by GC–MS (Loreto *et al.* 1996). However, because this fragment contains only seven of the 10 total carbon atoms, a quantitative understanding of monoterpene carbon sources remains to be determined. Using $^{13}CO_2$ labeling analysis, we quantified tropical monoterpene carbon sources of light-dependent leaf monoterpene emissions, and found a strong dependence on a recently photosynthesized substrate (Croteau & Purkett, 1989) (Fig. 2). These results are consistent with the current view that monoterpenes are produced via the methylerythritol 4-phosphate (MEP) pathway in plant chloroplasts (Gleizes *et al.* 1980; Jones *et al.* 2012). This indicates that global emission models should employ a photosynthesis-linked algorithm for tropical monoterpene emissions, similar to that achieved previously for isoprene (Unger *et al.* 2013). However, similar to isoprene (Jardine *et al.* 2014; Jardine *et al.* 2016), tropical monoterpene emissions should be linked to gross carbon assimilation processes rather than net carbon assimilation as an uncoupling of monoterpene leaf emissions from net photosynthesis was observed at high temperatures. As for isoprene, this may be due to the stimulation of leaf internal CO_2 sources at high temperatures, such as respiration and photorespiration, which reduce the net flux of CO_2 and contribute to 'alternate' carbon sources for monoterpene biosynthesis (Jardine *et al.* 2014).

Further, we demonstrate that, in contrast to landscape and regional emission model predictions (Fig. 6), the composition of leaf monoterpene emissions in the tropics is highly sensitive to leaf temperature. As maximum mid-day leaf temperatures increased throughout the 2015 dry season associated with a strong El Niño event, total ambient monoterpene concentrations above the primary rain forest also increased. This was
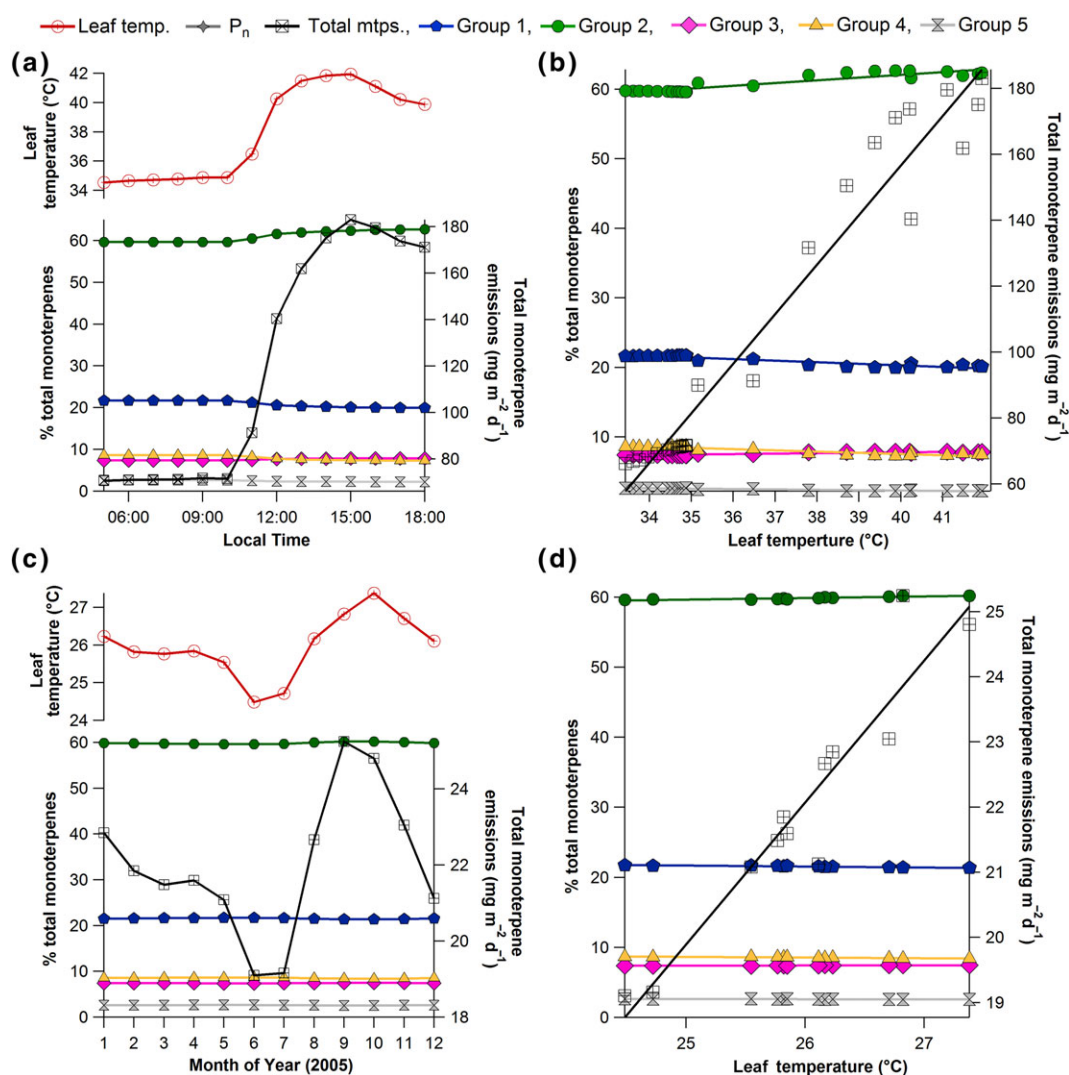
Figure 6. Coupled MEGAN 2.1-CLM 4.5 model estimates of monoterpene emissions from the central Amazonia. (a) Landscape scale hourly averaged leaf temperature with monoterpene emissions and composition (Groups 1–5 monoterpene emissions, % total) for a 12-h period during September 2008. (b) Landscape scale monoterpene emissions and composition leaf temperature sensitivities. (c) Regional scale monthly averaged vegetation temperature with monoterpene emissions and composition for the year 2005. (d) Regional scale monoterpene emissions and composition vegetation temperature sensitivities. See Table 1 for slopes and linear R^2 coefficients of determination for (b) and (d). [Colour figure can be viewed at wileyonlinelibrary.com]

associated with an increase in the fraction of Group 1 monoterpenes and a corresponding decrease in Groups 2–4 monoterpenes (Fig. 5). Similar temperature sensitivities were observed at the leaf level under controlled (Fig. 3) and natural diurnal temperature variations (Fig. S2). Given their higher reactivities with oxidants relative to other monoterpenes (Jardine *et al.* 2015), Group 1 monoterpenes may increase in both biological and atmospheric importance during climate warming extremes. Consistent with their well-documented roles in plant stress response (Fäldt *et al.* 2003), β-ocimenes may enhance the thermotolerance of photosynthesis and lead to increased monoterpene oxidation rates in the tropical boundary layer with potentially important consequences for cloud formation and water recycling. This highlights the need to include the temperature sensitivity of leaf monoterpene emission composition in future Earth system models. Current

'State of the art' monoterpene emission algorithms do not contain a function to represent monoterpene species composition variability, but rather focus on temperature and light dependent emission algorithms for total monoterpenes (Schurgers *et al.* 2009).

In *Arabidopsis thaliana*, an AtTPS03 (*E*)-β-ocimene synthase has been identified that produces a blend of acyclic, cyclic and bicyclic monoterpenes (Bohlmann *et al.* 2000; Fäldt *et al.* 2003). This blend of monoterpene products is similar to that observed from leaf emissions from *Q. ilex* in the Mediterranean (Staudt & Bertin, 1998) and leaf/landscape emissions in central Amazonia (Jardine *et al.* 2015). Furthermore, leaf-level Amazon surveys showed (*E,Z*)-β-ocimene as common monoterpenes emitted from hyperdominant tree genera (Jardine *et al.* 2015), leading to the hypothesis considered here, that an (*E,Z*)-β-ocimene family of monoterpene synthase enzymes

may be an important source of tropical leaf monoterpene emissions. According to the proposed mechanism for monoterpene biosynthesis (Chen *et al.* 2011; Degenhardt *et al.* 2009) (Fig. 1), several explanations exist for the high temperature sensitivity of leaf monoterpene emission composition. For example, a kinetic advantage of Group 1 production may exist because only one carbocation intermediate (geranyl cation) is required, followed by a proton abstraction. In contrast, multiple (3–4) carbocation intermediates are required to produce the cyclic and bicyclic monoterpenes of Groups 2–5. High leaf temperatures may also impede the enzymatic cyclization of GPP by lowering the stability of carbocation intermediates. While the presence of several distinct leaf monoterpene synthase enzymes operating in parallel with different temperature optima may also be considered, the presence of a *β*-ocimene synthase (Schwab, 2003) with high yields of Group 1 monoterpenes at elevated leaf temperatures is suggested by the Amazon field data. At high leaf temperatures, *β*-ocimenes dominated leaf (Fig. S4) and landscape emissions (Fig. 5 and S2). Nonetheless, detailed biochemical investigations are needed to determine the enzymatic mechanisms leading to the observed temperature sensitivity of tropical monoterpene emission composition.

Volatile isoprenoid emissions (including isoprene and monoterpenes) from plants can represent a major loss of carbon and energy resources (Jardine *et al.* 2015) with growing evidence supporting a functional role as antioxidants protecting photosynthesis from abiotic stressors like high light intensity and temperature (Loreto *et al.* 1998; Vickers *et al.* 2009). Isoprene protection of photosynthesis under high temperature stress has been discussed in terms of excess consumption of photosynthetic energy and reducing equivalents during biosynthesis which reduce the formation of ROS (Morfopoulos *et al.* 2014), direct isoprene-ROS antioxidant reactions (Jardine *et al.* 2012; Jardine *et al.* 2013) and signaling mechanisms mediated by isoprene oxidation products including defense gene activation (Karl *et al.* 2010). Limited studies suggest that monoterpenes also protect photosynthesis under abiotic stress (Peñuelas & Llusià, 2002; Peñuelas & Munné-Bosch, 2005; Vickers *et al.* 2009). Our observations, demonstrating the utilization of recently assimilated carbon for monoterpene biosynthesis and the high temperature sensitivity of monoterpene composition, support an important role of monoterpenes in thermotolerance of photosynthesis in the tropics. High leaf temperatures are well known to stimulate the overproduction of ROS (Hasanuzzaman *et al.* 2013), whose damaging effects may be mitigated both through increased monoterpene biosynthesis (excess photosynthetic energy consumption) and the fraction of monoterpene production that is highly reactive with ROS. Acyclic Group 1 monoterpenes are hundreds of times more reactive with ROS than isoprene and cyclic and bicyclic monoterpenes of Groups 2–5 (Arey *et al.* 1990; Atkinson & Arey, 2003; Jardine *et al.* 2015). Given the demonstrated ability of isoprene to mitigate the overproduction of ROS in leaves under high temperature stress and its associated oxidative damage like membrane peroxidation (Velikova & Loreto, 2005), we speculate that highly reactive monoterpenes (e.g., Group 1) play a similar, but potentially more effective role. Thus, the high temperature sensitivity of Group 1

monoterpene emission composition (4.4% $°C^{-1}$) may represent a new quantitative 'thermometer' of tropical forest oxidative stress observable across a wide range of temporal and spatial scales. By acting as more effective leaf antioxidants, highly reactive Group 1 monoterpenes may play an important role in the thermotolerance of tropical photosynthesis to elevated temperatures associated with drought. Following rapid atmospheric oxidation in the boundary layer, forest emissions of highly reactive Group 1 monoterpenes may enhance secondary organic aerosol and cloud condensation nuclei formation/growth. These processes may enhance cloud cover, reduce leaf temperature and increase precipitation recycling, and therefore represent an effective biosphere-atmosphere negative feedback to warming. We conclude that this monoterpene 'thermometer' will be a useful tool as a new signal of coupled tropical forest-atmosphere oxidative response to climate warming and its associated changes in terrestrial carbon and water cycling.

Supplementary information available

Supplementary information is available for download including individual files for field site locations and modeling boundaries (figS. 3.kmz file), observational and derived data (Igor Professional files), monoterpene temperature sensitivities (MS Excel files) and supplementary Figures (S1–S4). Four supplementary figures can be found in the supplementary information document (.pdf file) including Figure S1: Example extracted ion chromatogram (m/z = 93) from the ambient air showing the presence of 11 different monoterpenes above the upper canopy (27 m) in central Amazonia, Figure S2: Example of natural diurnal patterns from main canopy (25.5 m) *P. anomala* leaves on 12 September 2015 in central Amazonia, Figure S3: Map of AIRS data boundaries and MEGAN 2.1 – CLM 4.5 modeling boundaries, and Figure S4: Example m/z 93 extracted ion GC–MS chromatograms showing monoterpenes emitted from a banana leaf (*Musa* sp.) as a function of temperature, and *P. anomala* canopy leaves under naturally varying conditions of light and leaf temperature.

REFERENCES

Arey J., Atkinson R. & Aschmann S.M. (1990) Product study of the gas-phase reactions of monoterpenes with the OH radical in the presence of NOx. *Journal of Geophysical Research: Atmospheres (1984–2012)* **95**, 18539–18546.

Atkinson R. & Arey J. (2003) Gas-phase tropospheric chemistry of biogenic volatile organic compounds: a review. *Atmospheric Environment* **37**, 197–219.

Bohlmann J., Martin D., Oldham N.J. & Gershenzon J. (2000) Terpenoid secondary metabolism in *Arabidopsis thaliana*: cDNA cloning, characterization, and functional expression of a myrcene/(E)-β-ocimene synthase. *Archives of Biochemistry and Biophysics* **375**, 261–269.

Brienen R.J., Phillips O.L., Feldpausch T.R., Gloor E., Baker T.R., Lloyd J., … Zagt R.J. (2015) Long-term decline of the Amazon carbon sink. *Nature* **519**, 344–348.

Chambers J., Davies S., Koven C., Kueppers L., Leung R., McDowell N., Norby R. & Rogers A. (2014) Next Generation Ecosystem Experiment (NGEE) Tropics. *US DOE NGEE Tropics white paper*.

Chen F., Tholl D., Bohlmann J. & Pichersky E. (2011) The family of terpene synthases in plants: a mid-size family of genes for specialized metabolism that is highly diversified throughout the kingdom. *The Plant Journal* **66**, 212–229.

Croteau R. & Purkett P.T. (1989) Geranyl pyrophosphate synthase: characterization of the enzyme and evidence that this chain–length specific prenyltransferase is associated with monoterpene biosynthesis in sage (*Salvia officinalis*). *Archives of Biochemistry and Biophysics* **271**, 524–535.

Degenhardt J., Köllner T.G. & Gershenzon J. (2009) Monoterpene and sesquiterpene synthases and the origin of terpene skeletal diversity in plants. *Phytochemistry* **70**, 1621–1637.

Fäldt J., Arimura G.-i., Gershenzon J., Takabayashi J. & Bohlmann J. (2003) Functional identification of AtTPS03 as (E)-β-ocimene synthase: a monoterpene synthase catalyzing jasmonate-and wound-induced volatile formation in *Arabidopsis thaliana*. *Planta* **216**, 745–751.

Feldpausch T., Phillips O., Brienen R., Gloor E., Lloyd J., Lopez-Gonzalez G., … Álvarez D.E. (2016) Amazon forest response to repeated droughts. *Global Biogeochemical Cycles* **30**, 964–982.

Ghirardo A., Koch K., Taipale R., Zimmer I., Schnitzler J.P. & Rinne J. (2010) Determination of de novo and pool emissions of terpenes from four common boreal/alpine trees by $^{13}CO_2$ labelling and PTR-MS analysis. *Plant, Cell & Environment* **33**, 781–792.

Gleizes M., Pauly G., Bernard-Dagan C. & Jacques R. (1980) Effects of light on terpene hydrocarbon synthesis in *Pinus pinaster*. *Physiologia Plantarum* **50**, 16–20.

Guenther A., Hewitt C.N., Erickson D., Fall R., Geron C., Graedel T., … Zimmerman P. (1995) A global-model of natural volatile organic-compound emissions. *Journal of Geophysical Research-Atmospheres* **100**, 8873–8892.

Guenther A., Jiang X., Heald C., Sakulyanontvittaya T., Duhl T., Emmons L. & Wang X. (2012) The Model of emissions of gases and aerosols from nature version 2.1 (MEGAN2.1): an extended and updated framework for modeling biogenic emissions. *Geoscientific Model Development* **5**, 1471–1492.

Harley P., Eller A., Guenther A. & Monson R.K. (2014) Observations and models of emissions of volatile terpenoid compounds from needles of ponderosa pine trees growing in situ: control by light, temperature and stomatal conductance. *Oecologia* **176**, 35–55.

Hasanuzzaman M., Nahar K., Alam M.M., Roychowdhury R. & Fujita M. (2013) Physiological, biochemical, and molecular mechanisms of heat stress tolerance in plants. *International Journal of Molecular Sciences* **14**, 9643–9684.

Jardine A., Jardine K., Fuentes J., Martin S., Martins G., Durgante F., … Chambers J. (2015) Highly reactive light-dependent monoterpenes in the Amazon. *Geophysical Research Letters* **42**, 1576–1583.

Jardine K., Chambers J., Alves E.G., Teixeira A., Garcia S., Holm J., … Fuentes J.D. (2014) Dynamic balancing of isoprene carbon sources reflects photosynthetic and photorespiratory responses to temperature stress. *Plant Physiology* **166**, 2051–2064.

Jardine K., Henderson W., Huxman T. & Abrell L. (2010) Dynamic solution injection: a new method for preparing pptv–ppbv standard atmospheres of volatile organic compounds. *Atmospheric Measurement Techniques* **3**, 1569–1576.

Jardine K.J., Abrell L., Jardine A., Huxman T., Saleska S., Arneth A., … Goldstein A. (2012) Within-plant isoprene oxidation confirmed by direct emissions of oxidation products methyl vinyl ketone and methacrolein. *Global Change Biology* **18**, 973–984.

Jardine K.J., Jardine A.B., Souza V.F., Carneiro V., Ceron J.V., Gimenez B.O., … Chambers J.Q. (2016) Methanol and isoprene emissions from the fast growing tropical pioneer species *vismia guianensis* (aubl.) pers. (hypericaceae)
in the central Amazon forest. *Atmospheric Chemistry and Physics* **16**, 6441–6452.

Jardine K.J., Meyers K., Abrell L., Alves E.G., Serrano A.M., Kesselmeier J., … Vickers C. (2013) Emissions of putative isoprene oxidation products from mango branches under abiotic stress. *Journal of Experimental Botany* **64**, 3697–3709.

Jones R., Ougham H., Thomas H. & Waaland S. (2012) Molecules, metabolism and energy. In *The Molecular Life of Plants*, pp. 42–73. Wiley-Blackwell, Chichester, West Sussex.

Karl T., Fall R., Rosenstiel T.N., Prazeller P., Larsen B., Seufert G. & Lindinger W. (2002) On-line analysis of the $^{13}CO_2$ labeling of leaf isoprene suggests multiple subcellular origins of isoprene precursors. *Planta* **215**, 894–905.

Karl T., Harley P., Emmons L., Thornton B., Guenther A., Basu C., Turnipseed A. & Jardine K. (2010) Efficient atmospheric cleansing of oxidized organic trace gases by vegetation. *Science* **330**, 816–819.

Kavouras I.G., Mihalopoulos N. & Stephanou E.G. (1999) Secondary organic aerosol formation vs primary organic aerosol emission: In situ evidence for the chemical coupling between monoterpene acidic photooxidation products and new particle formation over forests. *Environmental Science & Technology* **33**, 1028–1037.

Laan-Luijkx I., Velde I., Krol M., Gatti L., Domingues L., Correia C., … Kaiser J. (2015) Response of the Amazon carbon balance to the 2010 drought derived with CarbonTracker South America. *Global Biogeochemical Cycles* **29**, 1092–1108.

Lewis S.L., Brando P.M., Phillips O.L., van der Heijden G.M. & Nepstad D. (2011) The 2010 Amazon drought. *Science* **331**, 554–554.

Loreto F., Ciccioli P., Cecinato A., Brancaleoni E., Frattoni M., Fabozzi C. & Tricoli D. (1996) Evidence of the photosynthetic origin of monoterpenes emitted by *Quercus ilex* L. leaves by ^{13}C labeling. *Plant Physiology* **110**, 1317–1322.

Loreto F., Förster A., Dürr M., Csiky O. & Seufert G. (1998) On the monoterpene emission under heat stress and on the increased thermotolerance of leaves of *Quercus ilex* L. fumigated with selected monoterpenes. *Plant, Cell & Environment* **21**, 101–107.

Loreto F. & Velikova V. (2001) Isoprene produced by leaves protects the photosynthetic apparatus against ozone damage, quenches ozone products, and reduces lipid peroxidation of cellular membranes. *Plant Physiology* **127**, 1781–1787.

Marengo J.A., Tomasella J., Alves L.M., Soares W.R. & Rodriguez D.A. (2011) The drought of 2010 in the context of historical droughts in the Amazon region. *Geophysical Research Letters* **38** L12703.

Mittler R., Vanderauwera S., Suzuki N., Miller G., Tognetti V.B., Vandepoele K., … Van Breusegem F. (2011) ROS signaling: the new wave? *Trends in Plant Science* **16**, 300–309.

Morfopoulos C., Sperlich D., Peñuelas J., Filella I., Llusià J., Medlyn B.E., … Prentice I.C. (2014) A model of plant isoprene emission based on available reducing power captures responses to atmospheric CO_2. *New Phytologist* **203**, 125–139.

Oleson K.W., Lawrence D.M., Gordon B., Flanner M.G., Kluzek E., Peter J., Levis S., Swenson S.C., Thornton E. & Feddema J. (2010) Technical description of version 4.0 of the Community Land Model (CLM).

Peñuelas J. & Llusià J. (2002) Linking photorespiration, monoterpenes and thermotolerance in Quercus. *New Phytologist* **155**, 227–237.

Peñuelas J. & Munné-Bosch S. (2005) Isoprenoids: an evolutionary pool for photoprotection. *Trends in Plant Science* **10**, 166–169.

Phillips O.L., Aragão L.E., Lewis S.L., Fisher J.B., Lloyd J., López-González G., … Quesada C.A. (2009) Drought sensitivity of the Amazon rainforest. *Science* **323**, 1344–1347.

Pöschl U., Martin S., Sinha B., Chen Q., Gunthe S., Huffman J., … Helas G. (2010) Rainforest aerosols as biogenic nuclei of clouds and precipitation in the Amazon. *Science* **329**, 1513–1516.

Schurgers G., Arneth A., Holzinger R. & Goldstein A. (2009) Process-based modelling of biogenic monoterpene emissions combining production and release from storage. *Atmospheric Chemistry and Physics* **9**, 3409–3423.

Schwab W. (2003) Metabolome diversity: too few genes, too many metabolites? *Phytochemistry* **62**, 837–849.

Singsaas E.L., Lerdau M., Winter K. & Sharkey T.D. (1997) Isoprene increases thermotolerance of isoprene-emitting species. *Plant Physiology* **115**, 1413–1420.

Staudt M. & Bertin N. (1998) Light and temperature dependence of the emission of cyclic and acyclic monoterpenes from holm oak (*Quercus ilex* L.) leaves. *Plant, Cell & Environment* **21**, 385–395.

Staudt M. & Lhoutellier L. (2011) Monoterpene and sesquiterpene emissions from *Quercus coccifera* exhibit interacting responses to light and temperature. *Biogeosciences* **8**, 2757–2771.

Topp G., Davis J. & Annan A.P. (1980) Electromagnetic determination of soil water content: measurements in coaxial transmission lines. *Water Resources Research* **16**, 574–582.

Unger N., Harper K., Zheng Y., Kiang N., Aleinov I., Arneth A., … Guenther A. (2013) Photosynthesis-dependent isoprene emission from leaf to planet in a global carbon-chemistry-climate model. *Atmospheric Chemistry and Physics* **13**, 10243–10269.

Velikova V. & Loreto F. (2005) On the relationship between isoprene emission and thermotolerance in Phragmites australis leaves exposed to high temperatures and during the recovery from a heat stress. *Plant, Cell & Environment* **28**, 318–327.

Vickers C.E., Gershenzon J., Lerdau M.T. & Loreto F. (2009) A unified mechanism of action for volatile isoprenoids in plant abiotic stress. *Nature Chemical Biology* **5**, 283–291.

Zeng N., Yoon J.-H., Marengo J.A., Subramaniam A., Nobre C.A., Mariotti A. & Neelin J.D. (2008) Causes and impacts of the 2005 Amazon drought. *Environmental Research Letters* **3**, 014002.

SUPPORTING INFORMATION

Additional Supporting Information may be found in the online version of this article at the publisher's web-site: